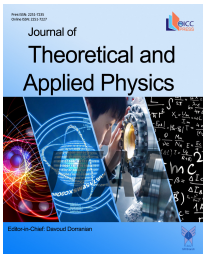

Volume 18, Issue 5, 182465 (1-10)

Journal of Theoretical and Applied Physics (JTAP)

https://dx.doi.org/10.57647/j.jtap.2024.1805.65

Modified polyamide membrane with TiO_2 nanoparticles, application for forward Osmosis, a molecular dynamics simulation study

Farrokh Roya Nikmaram*

Department of Chemistry, College of Basic Sciences, Yadegar-e-Imam Khomeini (RAH) Shahre Rey Branch, Islamic Azad University, Tehran, Iran.

*Corresponding author: nikmaram15@iau.ir

Original Research

Received:
3 July 2024
Revised:
10 September 2024
Accepted:
21 September 2024
Published online:
30 October 2024

Abstract:

Desalination of seawater is a significant challenge for arid regions and is the best way to obtain water resources. Today, many desalination methods are used, such as membrane desalination including reverse osmosis (RO) and forward Osmosis (FO). In forward Osmosis, unlike reverse Osmosis, energy consumption is much less and more economical. The various types of polymeric membranes are commonly used in the Osmosis processes such as polyamide (PA) polymer.
Polyamide (PA) membranes are known for their selective permeability to water and are extensively used in the seawater desalination. The use of non-toxic inorganic nanoparticles improves the polyamide membrane and increases its efficiency in the forward Osmosis process. This study investigates the efficiency of a modified polyamide membrane with different mole ratios of TiO_2 anatase nanoparticles in seawater desalination by using the molecular dynamics (*MD*) method during forward Osmosis simulation. The self-diffusion coefficients of water in forward Osmosis for PA membranes modified with 10^{-4}, 10^{-3}, 10^{-1}, and 1 wt% of TiO_2 were found to be 1.14, 1.11, 1.33 and 1.29×10^{-9} m^2s^{-1}, respectively. The membrane with 0.1% TiO_2 demonstrated a self-diffusion coefficient that aligns exceptionally well with the experimentally observed diffusion coefficient for the PA membrane in forward Osmosis.

Keywords: Polyamide; Self-diffusion coefficient; Forward Osmosis; Molecular dynamics; TiO_2

1. Introduction

One effective method for improving water quality is through membrane technology. Membrane modification preserves or increases its porosity so that water flux increases significantly and salt flux decreases [1–3].
Polymeric membranes are commonly utilized for water treatment in forward Osmosis processes. Numerous experimental studies have explored the performance of nanoparticle-modified membranes in Osmosis processes, with many findings published in the literature [4, 5].
Hybrid membranes leverage the benefits of various materials to enhance performance in Osmosis processes. By integrating multiple materials, such as polymers, ceramics, or nanoparticles, these membranes can improve selectivity, permeability, and durability compared to traditional ones [6]. This leads to higher efficiency, lower energy consumption, and better separation performance in processes like reverse Osmosis and forward Osmosis. Overall, hybrid membranes represent a promising approach to optimizing membrane performance and advancing Osmosis technology [7–11].
Polyamide hybrid membranes with materials such as ZnO [12], Fe_3O_4 [13] Al_2O_3 [14] and SiO_2 [15] have been used for the forward Osmosis process. In experimental research conducted by Park and colleagues, a polyamide thin film nanocomposite membrane modified with 0.25 wt% graphene oxide (GO) was used for forward Osmosis, with deionized water as the feed solution and a 0.5 M NaCl solution as the draw solution. The water flux performance was 19.77 $Lm^{-2}h^{-1}$ [16]. In 2021, Azadi and colleagues investigated the performance of an Al_2O_3. TiO_2 ceramic

membrane in forward Osmosis and concluded that hybrid membranes enhance membrane efficiency [17].
Titanium dioxide (TiO_2) nanoparticles added to a cellulose triacetate membrane and an aquaporin membrane have improved the water flux in forward Osmosis by 73.4% and 13.6% [18].
Hybrid membranes designed for water purification must be safe, non-toxic materials that maintain high water permeability.
Incorporating titanium dioxide (TiO_2) nanoparticles is an excellent choice due to their non-toxic nature and antifouling characteristics, which significantly enhance the membrane's hydrophilicity and overall performance. In a study conducted by Emadzadeh et al., a polyamide thin-film nanocomposite membrane used in forward Osmosis was enhanced with TiO_2 nanoparticles. The optimal water flux was achieved at a TiO_2 concentration of 0.6 wt%, resulting in a 33% improvement in forward Osmosis performance [19]. Additionally, various studies have shown that incorporating 0.5% TiO_2 into polysulfone [20] and 0.1% TiO_2 into PA [21, 22] can enhance forward Osmosis (FO) performance, achieving increases of 29.7% and 40%, respectively.
Forward Osmosis (FO) is garnering increased attention as a cost-effective method for water desalination. At the FO process, a semi-permeable membrane separates two solutions: pure water reservoir (the feed phase) and a concentrated salt solution (the draw solution). The spontaneous process allows water molecules to flow from the feed phase to the draw solution through the membrane, driven by the higher chemical potential of the feed solution. The forward Osmosis process does not require hydraulic pressure, making it an energy-efficient option. The concentration gradient between the two solutions is the driving force behind FO, which is favored for its higher water flux and low operational costs.
One of the important parameters in checking the performance of the osmotic membrane is the measurement of the water self-diffusion coefficient (D) in the membrane. This property has been obtained experimentally for many hybrid membranes. Experimental works of researchers show that the self-diffusion coefficient of water in polyamide membrane as one of the most important membranes at reverse Osmosis is equal to 0.6×10^{-9} m^2s^{-1} [23].
The self-diffusion coefficient of water in the forward Osmosis process of polyamide membrane modified with graphene quantum dots by molecular dynamics (MD) simulation, is 0.9×10^{-9} m^2s^{-1} [24].
In 2016, Wei et al. explored rapid water permeation pathways in aromatic polyamide membranes for reverse Osmosis using the molecular dynamics (MD) method. They found the diffusion coefficient of water to be approximately 5×10^{-9} m^2s^{-1} [1], corroborating the experimental findings of Durell et al., who reported a coefficient of 2.30×10^{-9} m^2s^{-1} [25].
This study aims to assess how different concentrations of titanium dioxide (TiO_2) in polyamide membranes affect forward Osmosis (FO) efficiency. Identifying the optimal TiO_2 concentration is crucial for maximizing water diffusion and minimizing ion passage, which could otherwise hinder FO performance. Understanding these pivotal factors can facilitate the selection of superior membranes for seawater desalination [26, 27].
To explore the trajectories of particles in multi-particle systems, molecular dynamics (MD) is an effective approach. This method employs Newton's equations of motion to simulate the interactions among particles, treating these interactions as force fields. The specific force field applied to each particle is contingent upon the nature of its adjacent particles and the characteristics of their interconnections [28, 29]. Recently, the application of MD has gained traction in the study of water transport through osmotic membranes, highlighting its versatility and effectiveness in such research.
Molecular dynamics simulation technique is a powerful tool for forecasting molecular characteristics such as diffusion, transmembrane transport of molecules, and the accumulation of particles adjacent to the membrane. This study delves into three key aspects: self-diffusion coefficients, radial distribution functions, and coordination numbers, all assessed through MD simulations. The self-diffusion coefficient (D) is especially crucial for estimating the diffusion rates of macromolecules in cellular biochemical activities and of the water molecules in osmotic operations.

2. Simulation method

In this research, we investigated the impact of incorporating titanium dioxide (TiO_2) into the polyamide membrane on the self-diffusion coefficient of water during forward Osmosis, using the molecular dynamics (MD) method.
The self-diffusion coefficient (D) is especially crucial for estimating the diffusion rates of macromolecules in cellular biochemical activities and of the water molecules in Osmotic operations. The self-diffusion coefficients (D) of molecules in a three-dimensional space are calculated from the slope of the mean square displacement (MSD) graphs of particles, as described by the Einstein equation, Eq. (1) [30–32].

$$D = \frac{\langle R(t)^2 \rangle}{6t} \tag{1}$$

where "t" is molecular dynamics simulation time.
MSD is calculated as the deviation of position of an atom i at time t, and is defined by Eq. (2).

$$MSD = \frac{1}{N} \sum_{i=1}^{N} |\Delta \mathbf{r}_l(t)|^2 \tag{2}$$

where N is the number of particles.
The radial distribution function (RDF) quantifies the average spatial distribution of particles relative to a reference particle, Fig. 1.
The RDF, denoted as $g(r)$, is a function of distance, r, beginning at zero and increasing to a peak corresponding to the distance defining the first coordination shell of particles around the reference particle.
Integrating of the RDF across the initial peak yields the mean number of particles, N_c, within the first coordination shell at a distance ($r = 2$ Å to $r = 4$ Å) See Eq. (3), where 0.02 is the distance of $g(r)s$ [33].

$$N_c = \int_{2\,\mathring{A}}^{4\,\mathring{A}} \left(\frac{g_{r_i} + g_{r_{i+1}}}{2}\right) \times 0.02 \tag{3}$$

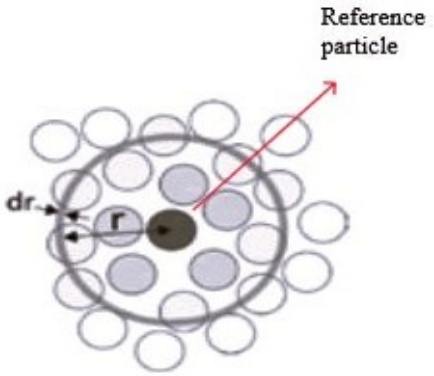

Figure 1. Distribution of particles relative to a reference particle.

This study contrasts its theoretical results with empirical data, focusing on the diffusion coefficient (D), which is commonly the sole parameter reported in experimental studies among the three parameters: diffusion coefficient (D), radial distribution function (RDF), and number of particles (N_c). The theoretical results of this work are compared with the experimentally determined diffusion coefficients from the other research. For computational analysis and property evaluation in molecular dynamics simulations, we used the Large-scale Atomic/Molecular Massively Parallel Simulator (LAMMPS) program [34].

Initially, three separate simulation cells of identical dimensions were created: a pure water cell, a salt solution cell, and a membrane cell saturated with water. Each cell underwent individual optimization. Subsequently, a 100 ps NPT simulation (constant moles (N), pressure (P), and temperature (T)) was performed at 300.0 K and 1 atm (10^{-4} GPa) to establish a new equilibrium and determine the updated density. The agreement between the calculated density and experimental values confirms the computational accuracy. Thereafter, the three cells were combined into layers to construct a comprehensive bulk system.

Both optimization and NPT calculations were performed on this combined structure.

To assess the transport properties of particles across the membrane, *MD* simulations were conducted at 300.0 K using the Grand Canonical Monte Carlo (GCMC) method within the NVT ensemble (a canonical ensemble with constant molecules (N), volume (V), and temperature (T)). The Nosé-Hoover thermostat and Berendsen Barostat were employed throughout the simulations to maintain the temperature at 300.0 K and pressure at 1 atm, respectively [35, 36]. In all of the simulations, the Forcite Molecular Dynamics calculation with condensed-phase optimized molecular potentials for atomistic simulation studies (COMPASS) force field was carried out to reach an equilibrium structure using canonical ensemble (NVT) at 50.0 ps of total simulation time and 50000 numbers of steps. The compass force field is suitable to calculate the diffusional properties of water molecules and ions [37, 38].

Water molecules were modeled using the non-polarizable and rigid TIP4P/2005 model which has been shown to accurately reproduce [39].

In the implementing of cell optimization calculations, electrostatic interactions with the Ewald method and van der Waals interactions were considered at a cut-off radius of 1.25 nm.

The periodic boundary conditions (PBC) were considered for simulation bulk in x and y directions.

3. Construction of cells

3.1 Construction of polyamide cell

The polymerization reaction between m-phenylenediamine (MPD) as an aromatic amine monomer and trimesoyl chloride (TMC) as an aromatic acyl chloride monomer leads to the production of polyamide, Fig. 2 [40].

In experimental literature, the preparation of polyamide (PA) involves varying the ratio of MPD to TMC from 5:1 to 20:1, with a significant excess of MPD monomers [41].

In the first step, the monomer of polyamide is constructed by connecting the nitrogen of a free amine group of MPD and the carbonyl carbon of a free acyl chloride group of TMC, Fig. 3. Next, the chain of polymer is constructed by randomly homo polymer technique, and put in the box and then cross-linked with excess amount of MPD in the vacuum via *MD* simulation in the NVT ensemble at 300.0 k.

The minimized polyamide membrane is saturated with water molecules by performing the Forcite *MD* calculation at 300.0 K using the Grand Canonical Monte Carlo (GCMC) method to obtain a minimized saturated membrane [35]. In several repeated steps, the water molecules are loaded into

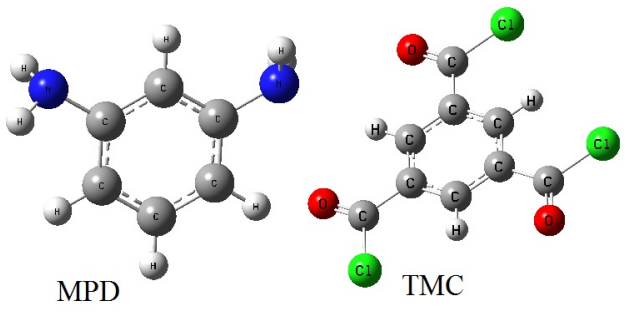

Figure 2. Structures of m-phenylenediamine (MPD) and 1, 3, 5-Benzenetricarbonyl trichloride (TMC).

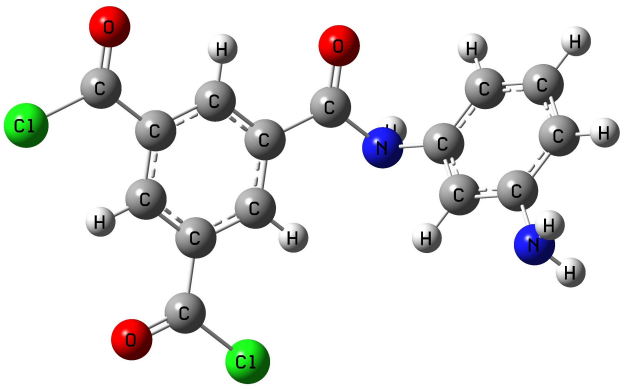

Figure 3. Monomer of polyamide.

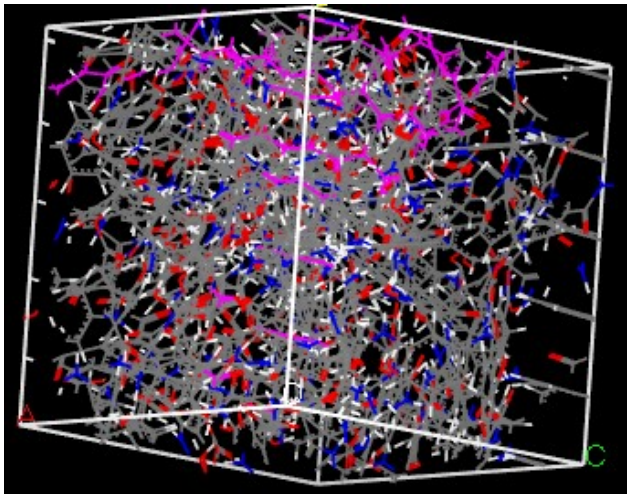

Figure 4. Cell of optimized polyamide membrane.
(Colors assigned to: red: oxygen; white: Hydrogen; blue: Nitrogen; gray: Carbon, green: Chlorine, Purple: Sodium)

the box of minimized polyamide membrane by adsorption locator calculation. After each step of loading, the energy of this box is calculated. The minimized saturated PA membrane is obtained with 175 water molecules. The cell of optimized saturated polyamide membrane with box parameters $(2.0 \times 2.0 \times 2.0)$ nm^3 shown in Fig. 4.
Table 1 shows the density of saturated polyamide membrane in equilibrated of the cell conditions.

3.2 Construction of H_2O cell

The water cell must match the PA membrane cell. Therefore, the lattice type of the water cell is adjusted to a cubic structure ($2.0 \times 2.0 \times 2.0$ nm^3) containing 268 water molecules. The number of water molecules is estimated based on the cell volume, the density of water (1 g/cm^3), and the molecular mass of water (18 g/mol). The H_2O reservoir reached equilibrium after optimization for 50.0 ps.

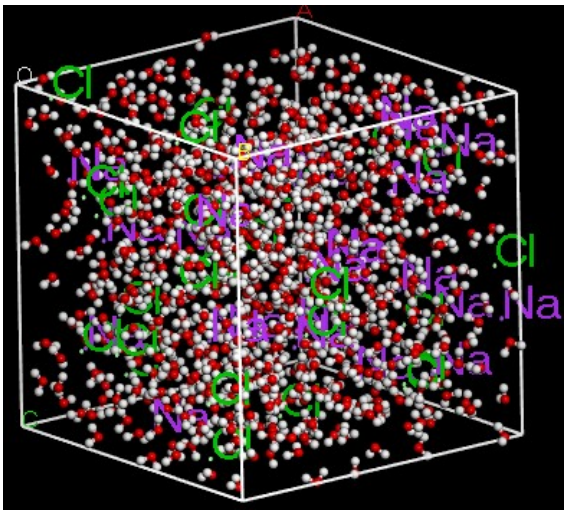

Figure 5. Salt solution cell.
(Colors assigned to: red: oxygen; white: Hydrogen; blue: Nitrogen; gray: Carbon, green: Chlorine, Purple: Sodium)

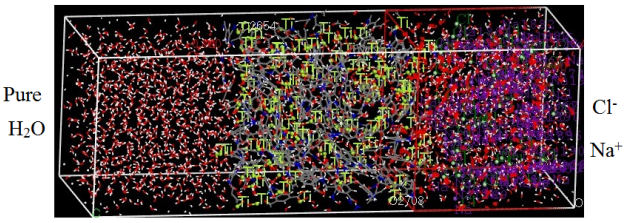

Figure 6. Simulation bulk with 10^{-4}% TiO_2.
(Colors assigned to: red: oxygen; white: Hydrogen; blue: Nitrogen; gray: Carbon, green: Chlorine, Purple: Sodium)

3.3 Construction of Na^+Cl^- solution cell

The reservoir of Na^+Cl^- solution with $(2.0 \times 2.0 \times 2.0)$ nm^3 dimension including 268 water molecules and 19Na^+ and 19Cl^- ions, corresponding to 23%wt of salt at concentration approximating seawater, Fig. 5, [42].
The geometry optimization calculation was carried out for salt solution cell at 50.0 ps of total simulation time and 50000 numbers of steps by using NVT canonical ensemble.

3.4 Simulation bulk

As illustrated in Fig. 6, the simulation bulk consists of a membrane cell surrounded by two cells: a NaCl salt solution cell on the right side and a pure water cell on the left side. Each cell has a cubic size of $2.0 \times 2.0 \times 2.0$ nm^3, and the dimensions of the bulk are $2.8 \times 2.8 \times 8.6$ nm^3 (Table 1).
In Fig. 6 can be see a snapshot of the NVT simulation bulk.
Table 1 shows the density of saturated polyamide membrane in equilibrated conditions of cell.

4. Results

In this study, we detail the outcomes of *MD* simulations analyzing the diffusion patterns of water molecules and Na^+ and Cl^- ions through a polyamide membrane. The analysis utilizes self-diffusion coefficients, radial distribution functions, and concentration profiles. To ascertain computational precision, we compared the density results from NPT simulations of the saturated polyamide membrane under equilibrium conditions with findings from other studies. Our results indicate a density of 1.21 g cm^{-3} for the saturated polyamide (refer to Fig. 7, Table 1), which aligns with Salestan et al.'s reported value of 1.19 g cm^{-3} [26] and Wei et al.'s values of 1.28 g cm^{-3} [1] and 1.24 g cm^{-3} [43].

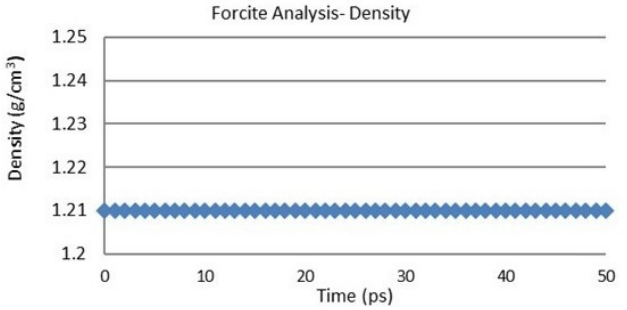

Figure 7. Density of saturated PA membrane.

Table 1. Density and lattice parameters of cells and bulk.

Cell	Density g cm^{-3}	Lattice parameters/nm^3
PA, Saturated membrane cell	1.21	$2.0 \times 2.1 \times 2.1$
Water cell	0.98	$2.1 \times 2.1 \times 2.1$
Salt solution cell	0.77	$2.0 \times 2.0 \times 2.0$
Bulk PA	0.80	$2.8 \times 2.8 \times 8.6$

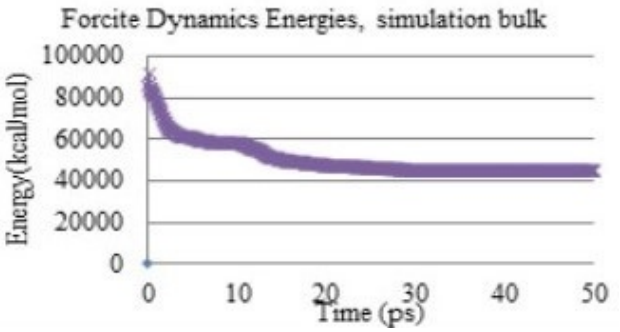

Figure 8. Energy minimization of bulk.

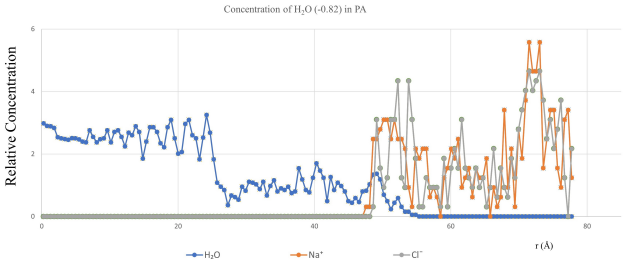

Figure 10. Relative concentration of pure H_2O at the initial times of calculation.

The average experimental density of hydrated polyamide (PA) is approximately 1.24 g cm^{-3} [44]. The consistency of our density results with these benchmarks suggests that the computational accuracy is within acceptable limits.

Fig. 8 shows that the bulk system reaches a minimum energy after 35 ps out of a total simulation time of 50 ps. The attainment of thermal equilibrium in the simulation bulk at 300.0 K is depicted in Fig. 9. The equilibrated system was then utilized to analyze water transport behavior. In the MD simulation, the system underwent a relaxation period of 50 ps, with analyses conducted using only the data from the final 20 ps.

During the NVT simulation, a net movement of water molecules was observed from the pure water cell (feed phase) to the salt solution cell (draw phase). This migration is driven by the chemical potential gradient between the two phases, consistent with the principles of forward Osmosis. A detailed examination of the water molecules' oxygen charges revealed a charge of -0.82 in molecules originating from the pure water source. In contrast, the oxygen charge in molecules from the salt solution source was found to be 0.0. The disparity in oxygen charges can be attributed to differences in the chemical environments and interactions with neighboring molecules.

The diffusion dynamics of water molecules and ions were investigated through concentration profile analysis. Following the minimization of the simulation bulk, we determined the relative concentration distributions of water molecules and ions along the z-axis. Figures 10 and 11 illustrate the relative concentrations of water, sodium, and chloride ions as functions of distance within the bulk system. At the left of chart, the relative concentration of pure water, carrying a charge of -0.82, is displayed for the pure water cell, while the right side presents the concentrations of sodium and chloride ions in the salt solution cell.

Fig. 10 reveals that the water concentration between 2.8 to 4.3 nanometers remains constant, indicating the membrane's saturation with water. Prior to initiating the calculations

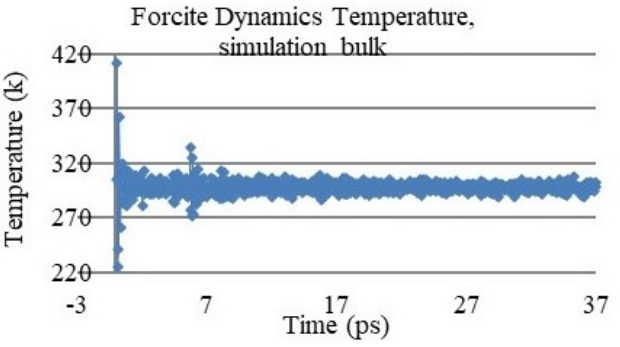

Figure 9. Temperature equilibrium of simulation bulk.

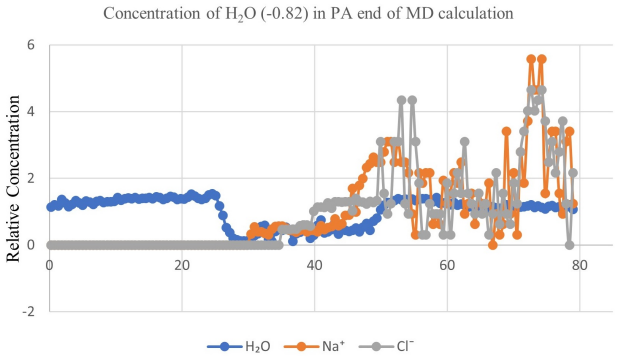

Figure 11. Relative concentration of pure H_2O at the end of calculation.

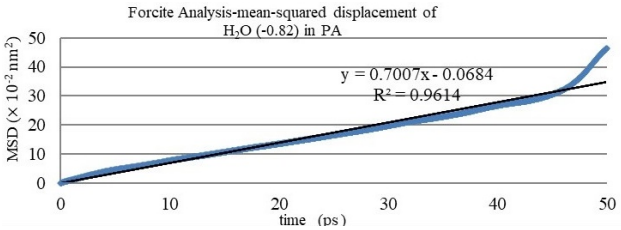

Figure 12. Mean-squared displacement of pure water in PA.

(as shown in Fig. 10), the concentration of water with a charge of -0.82 on the right side of the chart is nonexistent, indicating that water has not yet commenced its flow from the pure water to the salt solution side. As the calculations proceed, pure water molecules migrate into and through the membrane, evidenced by the increasing presence of water molecules with a charge of -0.82 on the membrane's right side. Upon completion of the calculations and the system's attainment of equilibrium (as depicted in Fig. 11), the concentration of these water molecules becomes roughly equivalent in both cells. Conversely, there is no detectable movement of Na^+ and Cl^- ions towards the left side of the bulk (the pure water cell), as demonstrated in Fig. 11.

Figures 12 and 13 show examples of *MSD* diagrams, displaying the mean-squared displacement (*MSD*) of pure water molecules (with an oxygen charge of -0.82) and Na^+ ions diffusing in the polyamide membrane, respectively, as a function of time.

The slop of *MSD* chart for pure H_2O is obtained 0.7×10^{-2} nm^2 ps^{-1} and for Na^+ 0.66×10^{-2} nm^2 ps^{-1}.

The self-diffusion coefficients (D) of water and Na^+ and Cl^- are determined from the slop charts of mean square displacement (*MSD*) in three dimensions (see Eq. (1) and Eq. (2)). The calculated self-diffusion coefficients (D) of pure water molecules and Na^+ and Cl^- ions in PA are 0.92×10^{-9} m^2 s^{-1} and 0.44×10^{-9} m^2 s^{-1}, 0.48×10^{-9} m^2 s^{-1} respectively.

By considering the charge differences of oxygen atoms in water across different regions, we obtained the radial distribution functions (RDFs) of pure water molecules and compared them with the RDF of H_2O in the salt solution (Fig. 14). The diffusion coefficient in the membrane varies, ranging from 2.63×10^{-1} nm to 4.19×10^{-1} nm for pure H_2O, with an average distribution of 28.4 at the main RDF peak. In contrast, for H_2O in the salt solution, the main RDF peak is at 0.97×10^{-1} nm with an average distribution of 25.0, indicating greater penetration of pure water into the membrane.

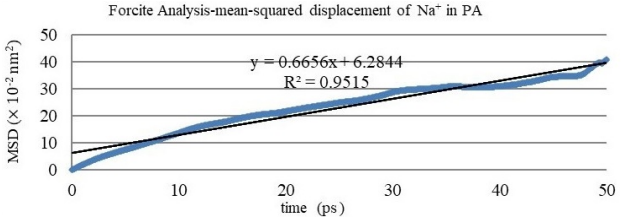

Figure 13. Mean-squared displacement of Na^+ in PA.

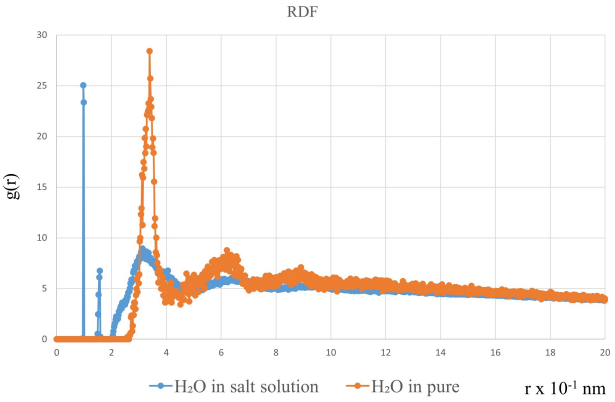

Figure 14. RDF diagram of H2O in PA bulk, pure H_2O and H_2O in salt solution.

Integration of the RDF diagram provides the relative number (N_c) of water molecules around the main peak of the RDF for pure H_2O, specifically between 0.2 nm and 0.4 nm (see Eq. (3)). Similarly, the relative number of ions is derived from RDF integration around their main peaks. The N_c results are listed in Table 2, showing values of 16.60, 13.62, and 12.46 for H_2O, Na^+, and Cl^- in PA, respectively. Only in pure PA and modified polyamide with 0.1% of TiO_2, the N_c for water is greater than sodium and chlorine ions. In other concentrations of TiO_2, N_c of water is lower than ions. This is one of the reasons that show that modification of polyamide with a concentration of 0.1% of TiO_2 is a better option for water passage.

The primary objective of this research is to examine how varying concentrations of titanium dioxide (TiO_2) influence water permeability. By incorporating TiO_2 into the membrane at different weight percentages, we conducted further analyses, the details of which are presented in Table 2.

Fig. 15 displays the self-diffusion coefficients (D) of water molecules and Na^+ and Cl^- ions at 300.0 K across various TiO_2 concentrations in polyamide (PA). It is evident that TiO_2 concentrations distinctly affect the diffusion coefficients. In this chart, the self-diffusion coefficient of water at a TiO_2 concentration of 0.1% is higher than at other concentrations. At a concentration of 1%, the self-diffusion coefficient of water is close to that at 0.1%, but this value is higher for sodium and chlorine ions.

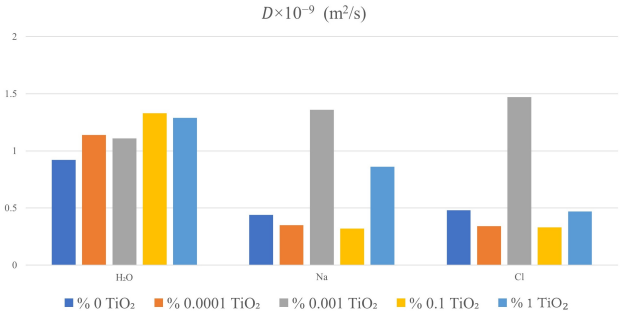

Figure 15. Self-diffusion coefficients (D) of water molecules and Na^+ and Cl^- at the different concentrations of TiO_2 in PA.

Table 2. Mean square displacement (*MSD*), diffusion coefficients (D), maximum of radial distribution function peak ($g(r)$) and coordination number (N_c) of membranes.

Weight percentages %TiO_2	*MSD* (10^{-2}nm^2 ps^{-1})			$D \times 10^{-9}$ (m^2 s^{-1})			Maximum $g(r)$			N_c (2Å to 4Å)		
in PA membrane	H_2O	Na^+	Cl^-	H_2O	Na^+	Cl^-	H_2O	Na^+	Cl^-	H_2O	Na^+	Cl^-
0	0.552	0.266	0.267	0.92	0.44	0.48	28.40	53.31	51.85	16.60	13.62	12.46
10^{-4}	0.700	0.209	0.206	1.14	0.35	0.34	28.40	40.93	43.18	36.01	39.76	44.23
10^{-3}	0.666	0.820	0.884	1.11	1.36	1.47	27.77	69.40	78.32	15.12	19.99	27.5
10^{-1}	0.799	0.192	0.198	1.33	0.32	0.33	32.50	21.10	24.6	42.35	22.70	20.86
1	0.778	0.630	0.285	1.29	0.86	0.47	27.07	159.5	138.77	34.03	46.93	35.02

Notably, the diffusion coefficient (D) of H_2O exhibited an increase across all TiO_2 concentrations, with increments of 24%, 21%, 44.5%, and 40% for 10^{-4}%, 10^{-3}%, 10^{-1}%, and 1% weight percentages, respectively.

The PA membrane with 0.1% wt of TiO_2 demonstrated the optimal diffusion coefficient for pure H_2O. At this concentration, the diffusion coefficients for Na^+ and Cl^- ions were also lower compared to other concentrations. This phenomenon is likely due to the optimal dispersion of TiO_2 at a 0.1% concentration within the PA membrane, enhancing its hydrophilicity and consequently facilitating greater H_2O diffusion.

These findings are corroborated by the experimental work of Amini and colleagues, who observed that adding 0.1% TiO_2 to the polyamide membrane led to a 40% increase in water transport through the membrane during forward Osmosis [21].

5. Conclusion

In this research, the effect of different concentration of TiO_2 in the polyamide membrane on the permeation rate of water molecules in the membrane was investigated using molecular dynamics method during forward Osmosis simulation as a spontaneous process. The results indicate that by adding TiO_2 to the polyamide membrane at concentrations of 0.1%wt and 1%wt, the self-diffusion coefficient of water has significantly increased. To enhance the efficiency of the membrane in the forward Osmosis process, with the increase in the self-diffusion coefficient of water, the self-diffusion coefficient of ions must decrease, which is evident at the 0.1 weight percent of TiO_2. Comparing the results of this theoretical work with the experimental works that have been done in this regard shows that the molecular dynamics method can be helpful in predicting the efficiency of hybrid membranes in the forward Osmosis process.

Authors contributions
Not applicable

Availability of data and materials
The datasets generated during the current study are available from the corresponding author.

Conflict of interests
The authors declare that they have no known competing financial interests or personal relationships that could have appeared to influence the work reported in this paper.

References

[1] T. Wei, L. Zhang, H. Zhao, H. Ma, M. S. J. Sajib, H. Jiang, and S. Murad. "Aromatic polyamide reverse Osmosis membrane: an atomistic molecular dynamic simulation.". *J. Phys. Chem. B.*, **120**:10311–10318, 2016. DOI: https://doi.org/10.1021/acs.jpcb.6b06560.

[2] T. Yoshioka, K. Kotaka, K. Nakagawa, T. Shintani, H. C. Wu, H. Matsuyama, Y. Fujimura, and T. Kawakatsu. "Molecular dynamics simulation study of polyamide membrane structures and RO/FO water permeation properties.". *Membranes*, **127**:1–17, 2018. DOI: https://doi.org/10.3390/membranes8040127.

[3] H. C. Wu, T. Yoshioka, K. Nakagawa, T. Shintani, T. Tsuru, D. Saeki, Y. R. Chen, K. L. Tung, and H. Matsuyama. "Water transport and ion rejection investigation for application of cyclic peptide

nanotubes to forward osmosis process: A simulation study.". *Desalination*, **424**:85–94, 2017. DOI: https://doi.org/10.1016/j.desal.2017.09.008.

[4] W. J. Lau, S. Gray, T. Matsuura, D. Emadzadeh, J. Paul Chen, and A. F. Ismail. "A review on polyamide thin film nanocomposite (TFN) membranes: history, applications, challenges and approaches. ". *Water Research*, **80**:306–324, 2015. DOI: https://doi.org/10.1016/j.watres.2015.04.037.

[5] M. Yan, Y. Xi, N. Jiang, Q. Li, S. Zheng, Y. Hu, Y. Liu, W. Bao, and M. Huang. "High-performance thin film composite forward osmosis membrane for efficient rejection of antimony and phenol from wastewater: characterization, performance, and MD-DFT simulation. ". *Journal of Membrane Science*, **703**:122847, 2024. DOI: https://doi.org/10.1016/j.memsci.2024.122847.

[6] Y. Wang, Z. Li, W. Fu, Y. Sun, and Y. Dai. "Core-Sheath CeO_2/SiO_2 nanofibers as nanoreactors for stabilizing sinter-resistant Pt, enhanced catalytic oxidation and water remediation. ". *Advanced Fiber Materials*, **4**:1278–1289, 2022. DOI: https://doi.org/10.1007/s42765-022-00177-0.

[7] M. Ding, A. Szymczyk, F. Goujon, A. Soldera, and A. Ghoufi. "Structure and dynamics of water confined in a polyamide reverse-osmosis membrane: a molecular-simulation study. ". *Journal of Membrane Science*, **458**:236–244, 2014. DOI: https://doi.org/10.1016/j.memsci.2014.01.054.

[8] A. Portavoce, I. Blum, K. Hoummada, D. Mangelinck, L. Chow, and J. Bernardini. "Original methods for diffusion measurements in polycrystalline thin films.". *Defect and Diffusion Forum*, **322**:129–150, 2012. DOI: https://doi.org/10.4028/www.scientific.net/DDF.322.129.

[9] A. Mansuri, M. Völkel, T. Feuerbach, J. Winck, A. W. P. Vermeer, W. Hoheisel, and M. Thommes. "Modified free volume theory for self-diffusion of small molecules in amorphous polymers. ". *Macromolecules*, **56**:3224–3237, 2023. DOI: https://doi.org/10.1021/acs.macromol.2c02451.

[10] S. Inukai, R. Cruz-Silva, J. Ortiz-Medina, A. Morelos-Gomez, K. Takeuchi, T. Hayashi, A. Tanioka, T. Araki, S. Tejima, T. Noguchi, M. Terrones, and M. Endo. "High-performance multi-functional reverse osmosis membranes obtained by carbon nanotube polyamide nanocomposite. ". *Scientific Reports*, **5**:13562, 2015. DOI: https://doi.org/10.1038/srep13562.

[11] M. M. Abo El-Fadl, A. H. M. El-Aassar, M. H. El-Sayed, and M. A. F. El-Sheikh. "Use of synthesized aromatic polyamide reverse Osmosis membranes doped NanoTiO_2 in water desalination. ". *Egyptian Journal of Pure and Applied Science*, **2**:009–016, 2011. DOI: https://doi.org/10.21608/EJAPS.2011.186259.

[12] S. Mansouri, S. Khalili, M. Peyravi, M. Jahanshahi, R. R. Darabi, F. Ardeshiri, and A. S. Rad. "Sublayer assisted by hydrophilic and hydrophobic ZnO nanoparticles toward engineered osmosis process.". *Korean J. Chem. Eng.*, **35**:2256–2268, 2018. DOI: https://doi.org/10.1007/s11814-018-0086-9.

[13] R. R. Darabi, M. Peyravi, M. Jahanshahi, and A. A. Q. Amiri. "Decreasing ICP of forward Osmosis (TFN-FO) membrane through modifying PES-Fe_3O_4 nanocomposite substrate. ". *Korean J. Chem. Eng.*, **34**:2311–2324, 2017. DOI: https://doi.org/10.1007/s11814-017-0086-1.

[14] W. Ding, Y. Li, M. Bao, J. Zhang, C. Zhang, and J. Lu. "Highly permeable and stable forward osmosis (FO) membrane based on the incorporation of Al_2O_3 nanoparticles into both substrate and polyamide active layer.". *RSC Adv.*, **7**:40311–40320, 2017. DOI: https://doi.org/10.1039/c7ra04046f.

[15] J. Tharayil and A. Manaf. "Effect of different inorganic draw solutes on SiNPs-TFN membrane for forward osmosis desalination.". *Int. J. Environ. Sci. Technol.*, **19**:289–298, 2022. DOI: https://doi.org/10.1007/s13762-020-03083-3.

[16] M. J. Park, S. Phuntsho, T. He, G. M. Nisola, L. D. Tijing, X. M. Li, G. Chen, W. J. Chung, and H. K. Shon. "Graphene oxide incorporated polysulfone substrate for the fabrication of flat-sheet thin-film composite forward osmosis membranes. ". *Journal of Membrane Science*, **493**:496–507, 2015. DOI: https://doi.org/10.1016/j.memsci.2015.06.053.

[17] F. Azadi, A. Karimi-Jashni, M. M. Zerafat, and S. Saadat. "Fabrication, optimization, and performance of a novel double-skinned Al_2O_3.TiO_2 ceramic nanocomposite membrane for forward osmosis application. ". *Environmental Technology & Innovation*, **22**:101423, 2021. DOI: https://doi.org/10.1016/j.eti.2021.101423.

[18] W. Xue, K. K. K. Sint, C. Ratanatamskul, P. Praserthdam, and K. Yamamoto. "Binding TiO_2 nanoparticles to forward osmosis membranes via MEMO–PMMA–Br monomer chains for enhanced filtration and antifouling performance. ". *RSC Advances*, **34**:2546–2549, 2018. DOI: https://doi.org/10.1039/c8ra03613f.

[19] D. Emadzadeh, W. J. Lau, T. Matsuura, A. F. Ismail, and M. Rahbari-Sisakht. "Synthesis and characterization of thin film nanocomposite forward osmosis membrane with hydrophilic nanocomposite support to reduce internal concentration polarization.". *Journal of Membrane Science*, **449**:74–85, 2014. DOI: https://doi.org/10.1016/j.memsci.2013.08.014.

[20] D. Emadzadeh, W. J. Lau, T. Matsuura, M. Rahbari-Sisakht, and A. F. Ismail. "A novel thin film composite forward osmosis membrane prepared from PSf–TiO_2 nanocomposite substrate for water desalination.". *Chemical Engineering Journal*, **237**:70–80, 2014. DOI: https://doi.org/10.1016/j.cej.2013.09.081.

[21] M. Amini, A. Rahimpour, and M. Jahanshahi. "Forward osmosis application of modified TiO_2-polyamide thin film nanocomposite membranes. ". *Desalination and Water Treatment*, **57**:14013–14023, 2016. DOI: https://doi.org/10.1080/19443994.2015.1065441.

[22] A. A. Mayyahi. "TiO_2 polyamide thin film nanocomposite reverses Osmosis membrane for water desalination.". *Membranes*, **8**:66, 2018. DOI: https://doi.org/10.3390/membranes8030066.

[23] Z. E. Hughes, C. J. Shearer, J. Shapter, and J. D. Gale. "Simulation of water transport through functionalized single-walled carbon nanotubes (SWCNTs).". *J. Phys. Chem. C.*, **116**:24943–24953, 2012. DOI: https://doi.org/10.1021/jp307679h.

[24] S. K. Salestan, S. F. Seyedpour, A. Rahimpour, A. A. Shamsabadi, A. Tiraferri, and M. Soroush. "Molecular dynamics insights into the structural and water transport properties of a forward Osmosis polyamide thin-film nanocomposite membrane modified with graphene quantum dots. ". *Ind. Eng. Chem. Res.*, **59**:14447–14457, 2020. DOI: https://doi.org/10.1021/acs.iecr.0c00330.

[25] S. R. Durell, B. R. Brooks, and A. Ben-Naim. "Solvent-Induced forces between two hydrophilic groups.". *J. Phys. Chem.*, **98**:2198–2202, 1994. DOI: https://doi.org/10.1021/ j100059a038.

[26] S. S. Shenvi, A. M. Isloor, and A. F. Ismail. "A review on RO membrane technology: developments and challenges. ". *Desalination*, **368**:10–26, 2015. DOI: https://doi.org/10.1016/j.desal.2014.12.042.

[27] M. A. Rayan and I. Khaled. "Seawater desalination by reverse osmosis (case study). ". *Desalination*, **153**: 245–251, 2002. DOI: https://doi.org/10.1016/S0011-9164(02)01143-8.

[28] M. Goudarzi and M. Gholipour Shahraki. "The influence of hydrogen and oxygen vacancy concentrations on diffusion coefficients of oxide and hydride ions in reduced barium titanate oxyhydride using molecular dynamics simulation.". *Physica B: Condensed Matter*, **678**:415784, 2024. DOI: https://doi.org/10.1016/j.physb.2024.415784.

[29] M. Tohidi and D. Toghraie. "The effect of geometrical parameters, roughness and the number of nanoparticles on the self-diffusion coefficient in Couette flow in a nanochannel by using of molecular dynamics simulation. ". *Physica B: Condensed Matter*, **518**:20–32, 2017. DOI: https://doi.org/10.1016/j.physb.2017.05.014.

[30] D. Hofmann, L. Fritz, J. Ulbrich, C. Schepers, and M. Bohning. "Detailed-atomistic molecular modeling of small molecule diffusion and solution processes in polymeric membrane materials. ". *Macromolecular Theory and Simulations*, **9**, 2000. DOI: https://doi.org/10.1002/1521-3919(20000701)9:6¡293::AID-MATS293¿3.0.CO;2-1.

[31] T. Thanh-Ha Nguyen. "Microstructural and dynamical heterogeneity characteristics in Al_2O_3-$2SiO_2$ liquid.". *VNU Journal of Science Mathematics-Physics*, **34**, 2018. DOI: https://doi.org/10.25073/2588-1124/vnumap.4231.

[32] X. Michalet. "Mean square displacement analysis of single-particle trajectories with localization error: brownian motion in an isotropic medium.". *Phys. Rev. E.*, **82**:041914, 2010. DOI: https://doi.org/10.1103/PhysRevE.82.041914.

[33] A. J. H. Frijns, C. C. M. Rindt, and S. V. Gaastra-Nedea. "Modeling thermochemical reactions in thermal energy storage systems.". *Advances in Thermal Energy Storage Systems (Second Edition)*, : 497–542, 2021. DOI: https://doi.org/10.1016/B978-0-12-819885-8.00017-6.

[34] S. Plimpton. "Fast parallel algorithms for short-range molecular dynamics. ". *J. Comput. Phys.*, **117**:1–19, 1995. DOI: https://doi.org/10.1006/jcph.1995.1039.

[35] P. Vo, H. Lu, K. Ma, J. Forsman, and C. E. Woodward. "Local grand canonical monte carlo simulation method for confined fluids. ". *Journal of Chemical Theory and Computation*, **15**:6944–6957, 2019. DOI: https://doi.org/10.1021/acs.jctc.9b00804.

[36] W. G. Hoover. "Canonical dynamics: equilibrium phase-space distributions. ". *Physical Review A*, **31**:1695–1697, 1985. DOI: https://doi.org/10.1103/physreva.31.1695.

[37] M. J. McQuaid, H. Sun, and D. Rigby. "Development and validation of COMPASS force field parameters for molecules with aliphatic azide chains. ". *Journal of Computational Chemistry*, **25**:61–71, 2004. DOI: https://doi.org/10.1002/jcc.10316.

[38] X. Wang, C. Tang, Q. Wang, X. Li, and J. Hao. "Selection of optimal polymerization degree and force field in the molecular dynamics simulation of insulating paper cellulose.". *Energies*, **14**:1–11, 2017. DOI: https://doi.org/10.3390/en10091377.

[39] J. L. F. Abascal and C. Vega. "A general- purpose model for the condensed phases of water: TIP4P/2005. ". *J. Chem. Phys.*, **123**:234505, 2005. DOI: https://doi.org/10.1063/1.2121687,15.

[40] H. F. Ridgway, J. Orbell, and S. Gray. "Molecular simulations of polyamide membrane materials used in desalination and water reuse applications: recent developments and future prospects. ". *Journal of Membrane Science*, **524**:436–448, 2017. DOI: https://doi.org/10.1016/j.memsci.2016.11.061.

[41] X. Song, J. M. Teuler, W. Guiga, C. Fargues, and B. Rousseau. "Molecular simulation of a reverse osmosis polyamide membrane layer. In silico synthesis using different reactant concentration ratios.". *Journal of Membrane Science*, **643**:120010, 2022. DOI: https://doi.org/10.1016/j.memsci.2021.120010.

[42] N. Voutchkov. "Introduction to reverse Osmosis desalination-A SunCam online continuing education course.". , 2010. DOI: https://doi.org/10.13140/RG.2.2.13908.60801.

[43] V. Kolev and V. Freger. "Hydration, porosity and water dynamics in the polyamide layer of reverse osmosis membranes: A molecular dynamics study.". *Polymer*, **55**:1420–1426, 2014. DOI: https://doi.org/10.1016/j.polymer.2013.12.045.

[44] Y. Song, M. Wei, F. Xu, and Y. Wang. "Molecular simulations of water transport resistance in polyamide RO membranes: Interfacial and interior contributions. ". *Engineering*, **6**:577–584, 2020. DOI: https://doi.org/10.1016/j.eng.2020.03.008.